frontiers in Materials

ORIGINAL RESEARCH
published: 12 February 2020
doi: 10.3389/fmats.2020.00020

The Effect of pH on the Preparation of Electrically Conductive and Physically Stable PANI/Sago Blend Film via *in situ* Polymerization

M. E. Ali Mohsin[1], *Nilesh K. Shrivastava*[1], *Agus Arsad*[1,2]*, *Norazah Basar*[3] and *Azman Hassan*[1]

[1] Enhanced Polymer Research Group, School of Chemical and Energy Engineering, Universiti Teknologi Malaysia, Skudai, Malaysia, [2] Faculty of Engineering, UTM-MPRC Institute for Oil and Gas (IFOG), Universiti Teknologi Malaysia, Skudai, Malaysia, [3] Department of Chemistry, Faculty of Science, Bahru, Malaysia

This study attempts to prepare electrically conductive and physically stable PANI/Sago starch films by a simple one-pot synthesis method using ultrasound irradiation technique. To attain physical stability of the prepared films, the pH of the PANI/Sago dispersion was varied (2, 4, 6, 7, 9, and 11 pH) before drying. The effect of pH on the structural properties (^{1}H NMR and FT-IR), electrical conductivity (E.C), optical properties (UV-VIS), and morphology (FE-SEM) of the blends was studied. ^{1}H NMR results revealed that at low pH (2 and 4), degradation of sago starch took place and as the pH increases, deprotonation of PANI takes place. The findings of ^{1}H NMR were ably supported by E.C results, which showed gradual decrease in conductivity until pH 7 and then a drastic drop was noticed for pH 9 and 11. UV-Vis findings reveals that, as the pH increases, PANI deprotonates from emeraldine salt form to emeraldine base form. The morphological results were complimentary with ^{1}H NMR and FT-IR, while revealing different morphologies: coral like morphology with voids in them for blends with pH 2 and 4; well-connected and smooth morphology for blends with pH 6 and 7; and well-connected but with loose flake like morphology for blends with pH 9 and 11. Overall, the PANI/Sago blend with pH 6 was found to be electrically conductive and physically stable.

Keywords: polyaniline, sago starch, oxidative polymerization, ultrasonic irradiation, pH

OPEN ACCESS

Edited by:
Guilherme Mariz de Oliveira Barra, Federal University of Santa Catarina, Brazil

Reviewed by:
Abu Zayed M. Saliqur Rahman, The Ohio State University, United States
Juliana Coatrini Soares, Universidade de São Paulo São Carlos, Brazil

***Correspondence:**
Agus Arsad
agus@cheme.utm.my

Specialty section:
This article was submitted to Polymeric and Composite Materials, a section of the journal Frontiers in Materials

Received: *30 July 2019*
Accepted: *20 January 2020*
Published: *12 February 2020*

Citation:
Ali Mohsin ME, Shrivastava NK, Arsad A, Basar N and Hassan A (2020) The Effect of pH on the Preparation of Electrically Conductive and Physically Stable PANI/Sago Blend Film via in situ Polymerization. Front. Mater. 7:20. doi: 10.3389/fmats.2020.00020

INTRODUCTION

Among various conjugated polymers, Polyaniline (PANI) in its doped form have attracted huge interest due to its potential applications in light-emitting diodes, batteries, electromagnetic shielding, antistatic coating, and gas sensors (Negi and Adhyapak, 2002; Persaud, 2005; Al-Thani et al., 2018; Kumar et al., 2018). However, low solubility of the doped PANI in most organic solvents, poor mechanical properties and strenuous processability in the doped state hinders the commercial expansion of PANI. Therefore, continuous efforts are being made to overcome these limitations. One such effort is the preparation of conducting PANI blends or composites. The advantage of this method is, it delivers the synergic combination of enhanced processability of the conventional polymers and electrical and redox properties of PANI (Jones et al., 2010). In last couple of decades

many researchers have reported on blending of PANI with different types of conventional polymers, such as polyacrylonitrile (Fryczkowska et al., 2017), polyvinyl alcohol (PVA) (Laska et al., 1997), polystyrene (PS) (Roichman et al., 1999), and starch (Saikia et al., 2010; Janaki et al., 2012), have been investigated. Starch has attracted our attention because of its ease of availability and is highly economical. There are many varieties of starch available, the one which is of our interest is native Sago starch obtained from palm trees, as it is abundantly available in east Asia and it's the least explored one. As any other starch, Sago is made of two glucoside macromolecules; amylose and amylopectin. Additionally, the combination of a natural fully non-toxic, biodegradable material with a synthetic and multifunctional PANI looks as a promising new direction in the field of advanced, functional materials preparation.

In most studies involving preparation of PANI blends or composites, PANI was used as filler material, which reduces the surface conductivity of the blend at micro level. Therefore, in order to prepare PANI blends with uniform and enhanced conductivity at micro level, researchers have opted for *in situ* polymerization technique (Lu et al., 2007; Arenas et al., 2014; Pour-Ali et al., 2014; Wang et al., 2017). In this regard we tried preparation of PANI/Sago blends using *in situ* polymerization technique. However, our preliminary results showed that the prepared PANI/Sago blend lacked good physical stability, which is due to the high acidity (<1 pH) of the polymerized PANI/Sago solution. The high acidity of the polymerized PANI/Sago solution may result in degradation of sago starch during drying process. The high acidity of the solution is due to the use of Hydrochloric acid (HCl) as dopant and Sulphuric acid (H_2SO_4) as a by-product of aniline polymerization. HCl and H_2SO_4, are strong acids (with pH < 2) having hygroscopic, volatile and corrosive properties, which reduces the chemical stability of the sago starch in the PANI/Sago blend (Kawano et al., 2006).

Based on literature, this limitation can be overcome by couple of methods: by using weak dopants (>4 pH; Nguyen et al., 2014); or by immersing the synthesized blends in test buffer solution of varying pH (pH2-pH11; Gill et al., 2007). However, such methods were found to be unsuccessful as oxidative polymerization of PANI using medium or weak dopants resulted in Polyaniline in fully reduced or fully oxidized state. This is because the oxidation state of PANI is dependent on pH (Lindfors and Ivaska, 2002). Thus, according to the acidity level of the solutions, polyaniline may exist in different stable forms: leucoemeraldine $(C_6H_4NH)n$—completely reduced, white or colorless; emeraldine $[(C_6H_4NH)_2(C_6H_4N)_2]n$—blue for the emeraldine base (EB), green for the emeraldine salt (ES); pernigraniline $(C_6H_4N)n$—completely oxidized, blue or violet (Huang et al., 1986; Lindfors and Ivaska, 2002). Out of all the three aforementioned forms of PANI, emeraldine form is the desirable as it is the conductive and the most stable form of PANI. The other method of immersing of blends in buffer solution was found to be expensive as it involves multiple steps for preparation of PANI blends and then immersing it in buffer solution. Thus, there exists a need to prepare PANI blend in ES form without effecting the chemical stability of the polymer using simple and economical technique.

Therefore, in this study attempt have been made to prepare PANI/Sago blend in conductive form without effecting the chemical stability of sago starch. In order to maintain the chemical stability of the polymerized PANI/Sago blend, aqueous solution of Sodium hydroxide (NaOH) was added to the PANI/Sago dispersion before drying, until the desired pH was attained. The addition of NaOH is expected to prohibit the degradation of sago starch, by reacting with Hydrochloric acid (HCl) and forming Sodium Chloride (NaCl) salt, thus resulting in chemically stable PANI/Sago blend. For that, this paper reports the *in situ* polymerization of PANI in presence of sago starch to prepare PANI/Sago blend by oxidative polymerization of aniline using HCl and Ammonium persulfate (APS) as dopant and oxidant, respectively. The effect of pH on the structure, morphology and electrical conductivity was investigated by means of FT-IR, NMR, UV-Vis, FE-SEM, and four-point probe technique. The successful preparation of this film will open new avenues in the field of electronic devices such as bio-sensors, bio-conductors, EMI/RF shielding, antistatic coating medical applications etc.

MATERIALS AND METHODS

Materials

Aniline and ammonium persulfate (APS) were obtained from Sigma Aldrich, Sago starch was supplied by Craun Research Sdn. Bhd. (Sarawak, Malaysia) and hydrochloric acid (HCl 1M) was procured from Tolsa.

Synthesis of PANI/Sago Blends

PANI/Sago blend was synthesized by oxidative polymerization of aniline in the presence of Sago starch. The synthesis was began by sonicating pre-cooled sago gel with HCl for certain period of time then measured amount of aniline was added. To this, freshly prepared oxidant ammonium persulfate (APS) was added dropwise at 30 ml/h (Jelmy et al., 2013). Based on the literature, the oxidant/monomer and oxidant/dopant mole ratio was chosen as 1 (Cao et al., 1989; Jelmy et al., 2013). Monomer to Sago ratio was 1, concentration of dopant acid (HCl) was 1 M and the synthesis was carried out for 1 h (Pron et al., 1988; Cao et al., 1989; Jelmy et al., 2013). During the reaction, the temperature of the ice bath was maintained at 0–3°C; this was done to avoid any secondary reactions. As the polymerization proceeded, the color of the solution changed to white through yellow, brown, and finally to green, which indicates the formation of PANI Emeraldine salt. Then the obtained dark green color solution was left undisturbed for 24 h for the completion of polymerization. After completion of polymerization, varying quantity of NaOH solution was added dropwise to PANI/Sago dispersion until desired pH (2, 4, 6, 7, 9, and 11 pH) was attained, while constantly stirring. The final solution with uniform dispersion was then deposited as a film on a flat glass support and kept for drying at 60°C in oven for 48 h. Complete list of samples prepared and parameters followed is shown in **Table 1**.

Characterization

The pH of PANI/Sago aqueous dispersion was varied with varying Normality of NaOH. The pH was measured using a Hanna HI 991001 pH meter. Electrical conductivity was measured by using four point probe Jandel meter (Model RM3000). Each measurement involves three different samples to ensure the repeatability and reproducibility of the results. FT-IR spectra in the wavelength range of 4000–400 cm^{-1} were recorded using Nicolet 170SX. ^{1}H NMR was obtained on a Bruker 400 spectrometer using deuterated dimethyl sulfoxide-d6 (DMSO) as solvent. Using Hitachi SU8020 field emission scanning electron microscopy (FESEM) at an accelerating voltage of 5 kV, morphological analysis of the blends was done. UV-Vis analysis was performed using Lambda 1050 UV-VIS/NIR spectrophotometer.

TABLE 1 | List of PANI/Sago blends prepared.

Sample label	pH
Neat PANI	0.7
Neat Sago	–
P/S 2	2
P/S 4	4
P/S 6	6
P/S 7	7
P/S 9	9
P/S 11	11

HCl was used as dopant; APS was used as oxidant; feed ratio of Aniline:Sago was 1:1; Sonication time was 1 h.

RESULTS AND DISCUSSION

Physical Assessment of PANI/Sago Films

The assessment of the physical consistency of the films was made up by establishing if the film was broken or not when tested in a hand traction trial at a distance of 1 cm. If the film was not broken, it overcame the consistency criterion and then its conductivity was tested. The diameter of the produced films was 4–5 cm, as shown in **Figure 1**. The other desirable features in film such as consistency, physical homogeneity, and flexibility were tested by visual inspection of the samples and performed 7 days after the making of the films which is the estimated amount of time for solvent total removal and therefore the sample is considered to be stable (Arrieta et al., 2011). As shown in **Figure 1**, blends P/S 2 and P/S 4 were found to be very brittle with spongy properties, due to the degradation of starch. Therefore, no stable films were formed for P/S 2 and P/S 4 blends, as Sago imparts the structural integrity to the blends. Similarly, the blend with highest pH was found to be brittle and shrunk, the reason for this can be understood by FT-IR and ^{1}H NMR analysis.

With the degradation of Sago, PANI becomes dominant in the blend and this leads to increase in the rigidity of the blend, because of the rigid nature of PANI, thus resulting in brittle blends. Only the blends P/S 6 and P/S 7 were found to produce stable and intact PANI/Sago films as shown in **Figure 1**. A crack appeared in P/S 7 film during the hand traction trial, as shown

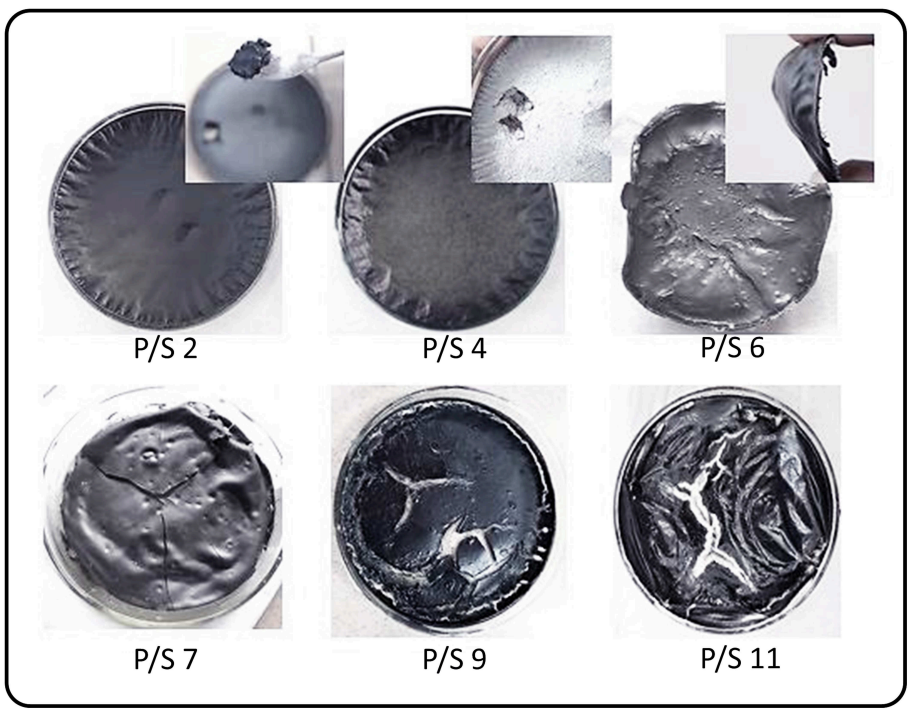

FIGURE 1 | Digital images of PANI/Sago films at different pH.

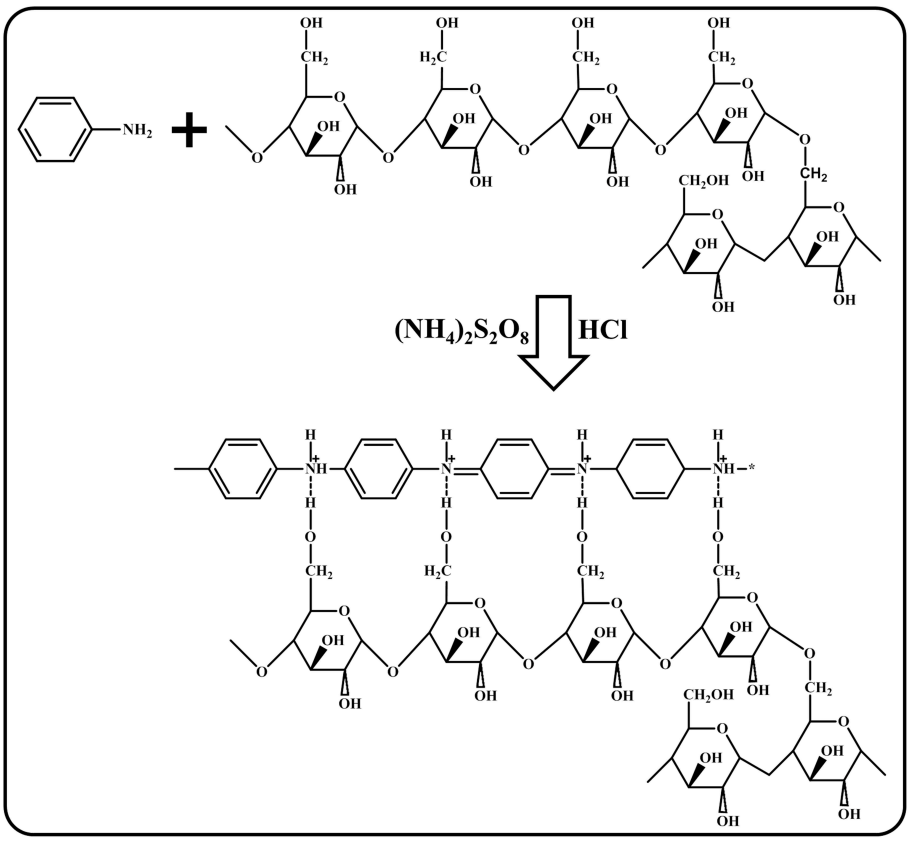

SCHEME 1 | Polymerization mechanism of PANI/Sago blend films.

in **Figure 1**. Whereas, P/S 6 film remains intact even after hand traction trial, shown in inset of **Figure 1**. This suggests film with pH 6 is smooth, stable, and ductile with protonated PANI attaching to the modified linear Sago starch structure and forms a strong hydrogen bond, as shown in **Scheme 1**.

Nuclear Magnetic Resonance (NMR)

The ^{1}H NMR spectrum of neat PANI, neat Sago and their blends at different pH are presented in **Figure 2**. The spectrum of neat PANI shows the characteristic peaks of doped PANI, which are: single peak in between 6.4 and 6.6 ppm, which is due to ($-NH_2$) end group (Wang et al., 2010). The presence of three sharp and equidistant peaks identified around 6.9–7.33 ppm (7.07, 7.20, and 7.33 ppm) with a coupling constant of 52 Hz, could be attributed to the proton related to nitrogen (Wang et al., 2010; Abdelkader et al., 2013). These triplet peaks are resulted from the ammonium protons, in other words, the triplet peak represents the doping protons of PANI, and these protons govern the conducting property of PANI (Abdelkader et al., 2013). The equal strength triplet could only be attributed to the proton related to nitrogen, since the ^{14}N (natural abundance: 99.62%) atom has a spin quantum number $I_N = 1$ (while $I_C = 0$), which makes it possible for the proton on ^{14}N to exhibit the triplet peaks with an integral area ratio of 1:1:1 in the ^{1}H NMR spectrum (Ning, 2000). The low intensity peaks at 1–2 ppm and at 8.15 ppm are due to the water protons bonded by (-NH-and-NH_2) groups, respectively (Kanungo et al., 2003), while the signals at 5.8 and 9.3 ppm are from –NH proton and hydrogen bonded –OH group, respectively (Lukasiewicz et al., 2014). **Figure 2** of neat sago shows the characteristic peaks of sago starch, which are: a triplet at 4.6, 5.1, and 5.4 ppm, respectively. The peak at 5.4 and 5.1 ppm belongs to (1–4) and (1–6) α- linkages of sago starch, respectively (Lukasiewicz et al., 2014).

In order to understand the effect of pH on PANI/Sago blends, it is best to analyse PANI and Sago peaks separately. Firstly, the impact of pH on PANI is analyzed, followed by sago starch. For simplicity same trend will be followed for rest of the paper.

The effect of incorporation of NaOH on the PANI is quite evident from the shift in the position of triplet peaks toward the downfield. As seen in **Figure 2** for PANI/Sago blend at 2 pH, the position of triplet is 7.0, 7.07, and 7.14 ppm, respectively. As the pH of the blend increases to 4, the position of triplet shifts to 6.9, 7.0, and 7.1 ppm and to 6.44, 6.62, and 6.80 ppm for PANI/Sago blend at 6 pH, respectively. Although the triplet peaks shifted toward downfield with increase in pH, it still remained equidistant, which is the characteristic of protonated PANI. The shifting of triplet could be due to interaction (hydrogen bonding) between PANI and sago. However, no triplet was observed for PANI/Sago blends with pH 7 and above, the disruption or disappearance of triplets in an indication of

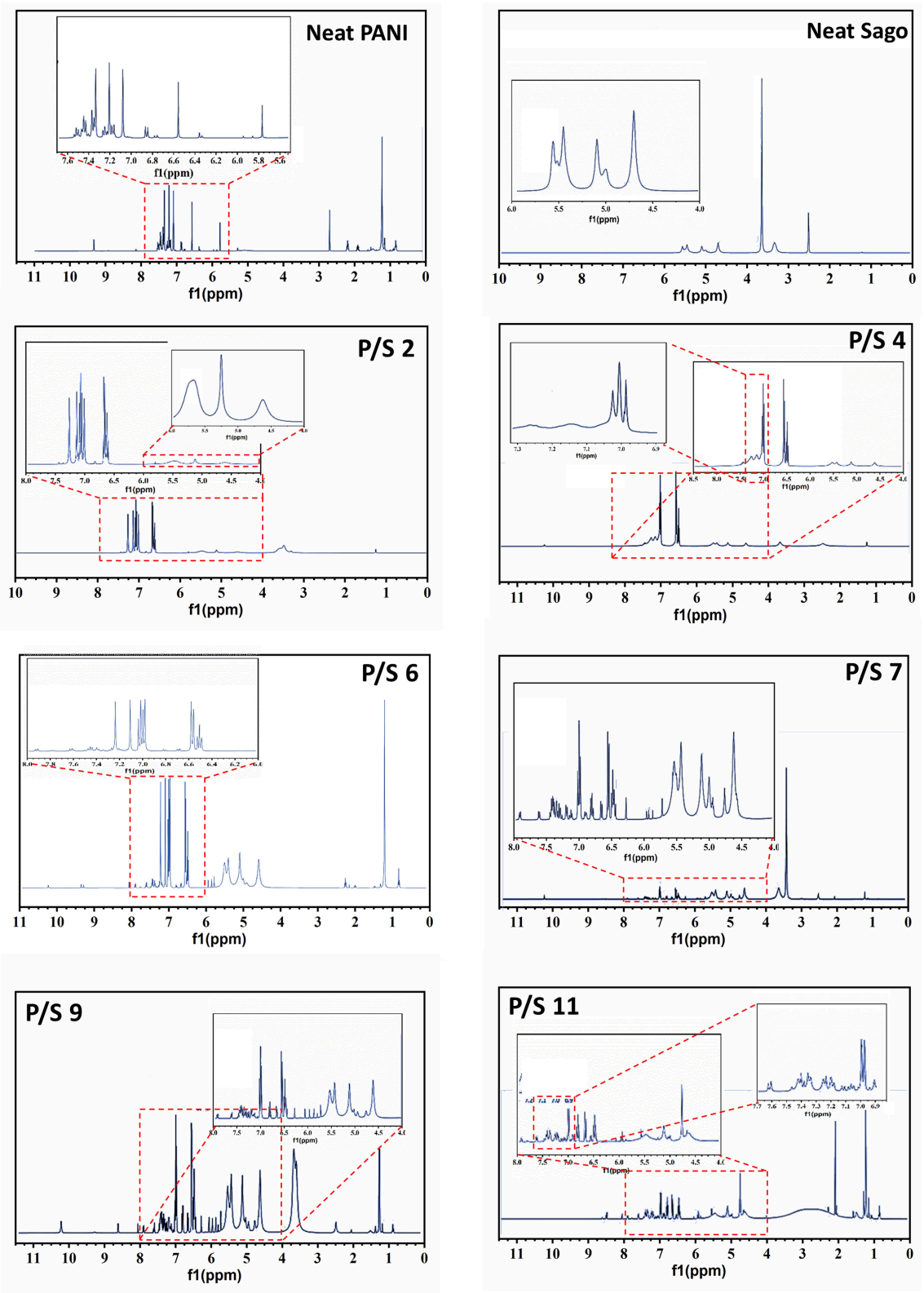

FIGURE 2 | ^{1}H NMR of Neat PANI, Neat Sago and PANI/Sago blends of varying pH.

change in oxidation state of PANI in PANI/Sago blends of the respective blends.

Further, as the pH of the blends increased to 9 and 11, the emergence of multiple new peaks between 5.5 and 6.5 ppm was observed, the arising of new peaks could be attributed to the alkaline oxidation of PANI/Sago blend (Beau et al., 1999; Venancio et al., 2006; Zujovic et al., 2008). Apart from peaks between 5.5 and 6.5 ppm, a new peak at 8.6 ppm was observed for blends with pH 9 and 11. The new peak located at 8.6 ppm is the characteristic peak of emeraldine base (EB) form of PANI, which is attributed to the NH groups of PANI-EB (Yamamoto and Moon, 1993). Thus, the appearance of new peak at 8.6 and disappearance of triplet for blends with pH 9 and 11, suggests change in form of PANI from ES to EB. These results are in agreement with the findings of Wang et al. (2010). Wang et al. reported comprehensively about the doping level of PANI and deprotonation of PANI when NaOH was added to it.

As shown in **Figure 2**, the characteristic peaks of Sago appears at 4.6, 5.1, and 5.4 ppm, respectively. It was observed that with change in pH of the PANI/Sago dispersion the intensity of these characteristic peaks of Sago also varied, suggesting structural modification of the blend. The intensity of Sago peaks increases with increase in pH of the Blend. For blends P/S 2 and P/S 4, the intensity of Sago peaks was found to be weak. Whereas, for blends with pH $\geq$ 6, the intensity of Sago peaks increases, as shown in **Figure 2**. The weak intensity of Sago is due to the degradation of Sago because of prolonged interaction of Sago with volatile acids (HCl and H_2SO_4) present in the PANI/Sago dispersion before eventually drying. This analysis is supported by the observations made during physical assessment of the blends after drying, as shown in the **Figure 1**. The increased intensity of Sago peaks for blends P/S 6, P/S 7, and P/S 9, suggests presence of Sago in the respective blends. For blends with pH $\geq$ 6, the PANI/Sago dispersion contains enough NaOH which reacts with HCl and forms NaCl salt, which restrain the degradation of Sago. Thus, for blends with pH $\geq$ 6 the chemical stability of Sago is maintained, which imparts physical stability to the blend. However, for P/S 11 blend the Sago peaks appears partially grown or beginning to diminish. The diminished peaks is a clear indication of the subjugation of Sago in the blend, thus suggesting partial degradation of Sago for P/S 11 blend.

Therefore, from this findings it can be said that, PANI/Sago blend with pH $<$ 6 are not desirable as they lack physical stability though they are protonated. Also, blends with pH $>$ 7 are not desirable as they contain new peak at 8.6 ppm which is the characteristic peak of emeraldine base (EB) form of PANI. Thus, blends with pH 6 and 7 were the only blends found to protonated and also physically stable. Further, evaluation of their E.C values and optical properties will help in understanding the degree of protonation of these blends.

Electrical Conductivity

Figure 3 shows the electrical conductivity of PANI/Sago blends at different pH values. The E.C of the neat PANI was found to be 1.78 Scm^{-1}. As observed from **Figure 3**, with the increase in pH of the solution the E.C value of the dried film decreases. A gradual decrease in the E.C was observed until pH 7. However,

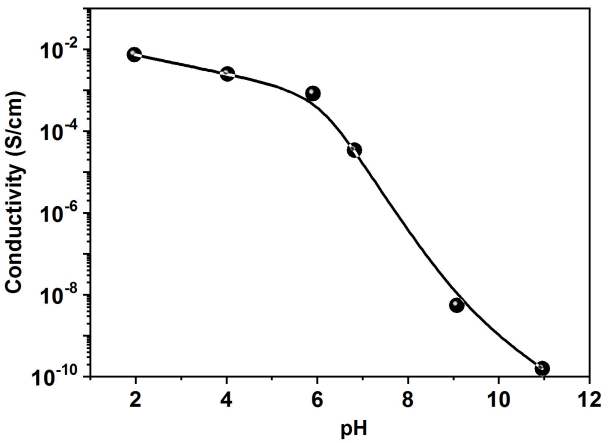

FIGURE 3 | Electrical conductivity of the PANI/Sago blend films at varying pH.

a drastic reduction can be noticed for PANI/Sago blends at pH 9 and pH 11.The PANI/Sago blend at pH 7 can still be considered as conductive [conductive plastic ranges up to 10^{-6} Scm^{-1} (Gulrez et al., 2014)], but the value is reduced by couple of folds as compare to PANI/Sago blend at pH 2, this could be due to deprotonation of PANI. Because once the conductive form of the PANI is formed, i.e., emeraldine salt, the addition of an acid or a base leads to protonation or deprotonation of the base (-NH-) sites in PANI, which causes switching of PANI between oxidation states (De Albuquerque et al., 2004). It is well-known fact that, the major contributor to the overall conductivity of polyaniline is the inter-chain charge transport (Wudl et al., 1987). Charge transport mechanism depends on a number of factors, protonation (doping level) being one of them. The relationship between doping and charge is well-explained by Huang and MacDiarmid as; Protonation/deprotonation of PANI results in an increase/decrease in the amount of charge on the polymer backbone, which results in increased/decreased conductivity (Huang and MacDiarmid, 1993). In another study by Shacklette (1994), the relationship between doping and charge is explained as; during the deprotonation of PANI, the interaction between PANI and polar molecule reduces, which induces redistribution of charge, resulting in reduced electrical conductivity. Thus, based on the aforementioned explanations, it can deduced that, when NaOH is added to the protonated PANI/Sago dispersion, deprotonation of PANI begins. The initial deprotonation of PANI results only in redistribution of charge, because at low pH, active sites for interaction between PANI and polar molecules are still present but in reduced quantity. Therefore, the gradual decrease in E.C of the blends with pH $\leq$ 7 suggests gradual reduction in active site on the polymer backbone. However, when the pH of the PANI/Sago dispersion increases (pH $>$ 7), the E.C of the blends falls drastically, suggesting elimination of all active sites on the polymer backbone. Which means no interaction between PANI and polar molecules takes place, thus resulting the deprotonation of PANI. The E.C and ^{1}H NMR results are complimentary to each other.

Ultraviolet–Visible Spectroscopy (UV-Vis)

In order to understand the effect of pH on PANI in PANI/Sago blends, UV-Vis analysis at different pH was carried out. As shown in **Figure 4**, neat PANI contains three absorption bands at around 358 nm, attributed to the π - π* transition in benzene rings; around 435 nm, attributed to exciton-couple π-polaron transition, and centered around 900 nm with a long tail is attributed to polaron - π* transition (Borah et al., 2014). These three absorption bands are the characteristic bands of doped PANI. From **Figure 4**, it can be confirmed that the band structure underwent a great change for PANI/Sago blends upon addition of NaOH. The change in band structure was more evident for blends with pH > 7.

Two different phenomenon were observed for, no major shifting of bands or drastic reduction in band intensities were observed for blends with pH ≤ 7. Whereas, for the blends with pH > 7, shifting of prominent bands and also disappearance of bands was noticed. For PANI/Sago blends with pH ≤ 7, the presences of PANI characteristic bands around 358, 435 nm and the appearance of polaron - π* transition absorption band in the region >750 nm confirms that P/S 2, P/S 4, P/S 6, and P/S 7 blends are in doped form. These results are consistent with the results reported in literature (Epstein et al., 1994; Kohlman et al., 1996; Lu et al., 2006; Soetaredjo et al., 2012).

However, for blends P/S 9 and P/S 11, a new absorption band appears around 650 nm, simultaneously resulting in the disappearance of the two absorption bands at around 435 and >750 nm. The disappearance of absorption bands at 435 and >750 nm and appearance of new band around 650 nm, indicates deprotonation of PANI. As seen in **Figure 4**, new set of absorption bands appears for P/S 9 and P/S 11 blends, two strong absorption bands at 337 and 690 nm for P/S 9 and 340 and 646 nm for P/S 11 was observed, respectively. These absorption bands for PANI/Sago blends for P/S 9 and P/S 11 blends are attributed to the formation of emeraldine base (Li and Wang, 2004; Lu et al., 2006). The emeraldine base form of PANI shows a low wavelength π - π* band and a strong absorption band around 600 nm attributed to a local charge transfer between a quinoid ring and the adjacent imine phenyl-amine units (intramolecular charge transfer exciton; Huang et al., 2002). The increase in pH of PANI/Sago blends leads to deprotonation of PANI in PANI/Sago blends and not to change in oxidation state, this can be confirmed by the position of absorption bands. As the reduced leucoemeraldine base form of PANI exhibits a band around 320 nm attributed to the π - π* electronic transition (Zhang et al., 2004). Pernigraniline base form of PANI shows two bands around 320 nm (π - π* band) and 530 nm (Peierl gap transition; Wallace et al., 2002). Thus, confirming increase in pH of PANI/Sago blends results in deprotonation of PANI from emeraldine salt form to emeraldine base form of PANI in PANI/Sago blends. These results are also complimenting the findings of ^{1}H NMR and E.C this far.

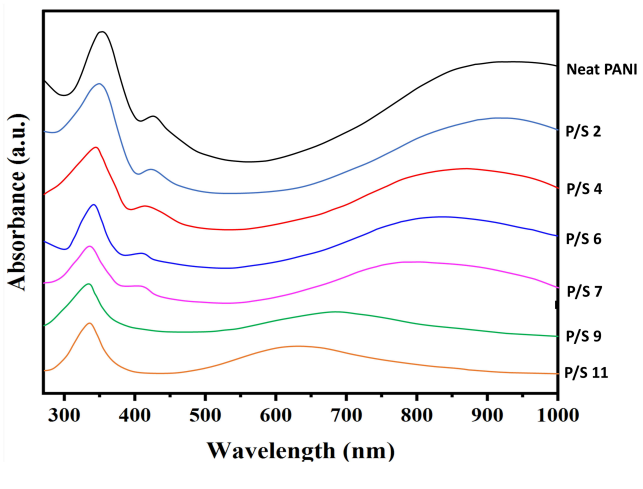

FIGURE 4 | UV-Vis spectrums of PANI, Sago and PANI/Sago blends of varying pH.

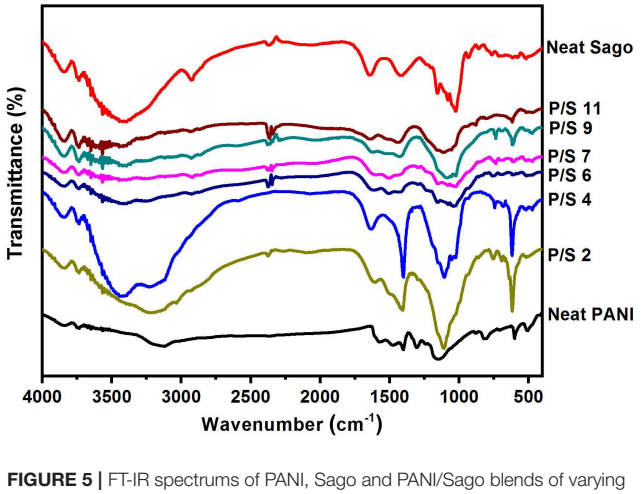

FIGURE 5 | FT-IR spectrums of PANI, Sago and PANI/Sago blends of varying pH.

Fourier Transform Infrared (FT-IR)

The effect of pH on the molecular structure of PANI/Sago blends are further analyzed using FT-IR. **Figure 5** of FT-IR allows to prove that the polymerization of aniline to PANI in presence of Sago starch took place successfully, irrespective of pH. The characteristic peaks of PANI occurring around 1,578, 1,490, 1,290, 1,240, 1,140, and 800 cm^{-1} corresponding to quinoid ring stretch, benzenoid ring stretch, N-H bend, asymmetric C-N stretch, −NH+ = stretch and aromatic C-H ring bend are shown in **Figure 5**, which are in agreement with those reported in literature (Tang et al., 1988; Ping, 1996; Kang et al., 1998). The peak around 800 cm^{-1} is the characteristic of para-substituted aromatic ring, through which the polymerization is expected to progress. The peak around 3,250–3,100 cm^{-1} is due to the presence of both the free N-H stretch and the O-H stretch from the polymer and the dopant acid, respectively (Jelmy et al., 2013). In the FT-IR spectra of neat Sago starch, characteristic peak between 1,035 and 1,156 cm^{-1} attributed to the C-O bond stretch in C-O-C of bonding, and peaks at 1,078 and 1,154 cm^{-1} attributed to C-O stretch in C-O-H bonding (Soetaredjo et al., 2012). Other absorption peak around 1,644 cm^{-1} corresponds to

the adsorbed water in the starch and bands around 1,420 cm^{-1} was ascribed to the angular deformation of C-H (Diop et al., 2011). Absorption around 3,700–3,000 cm^{-1} resulted from the vibration of the hydroxyl group (O–H) and (C–H) vibration stretch (Biswas et al., 2008; Diop et al., 2011).

An absorption band at 3,150 cm^{-1} in the spectrum of neat PANI is due to the absorption of free charge-carriers in the protonated polymer (Kang et al., 1998). It is one of the characteristic of a conducting form of PANI. This band slowly reduces in intensity and diminishes completely as the pH of the blend increases. As the pH increases to 2, the band at 3,150 cm^{-1} in PANI spectrum blue shifts to 3,196 cm^{-1} in P/S 2 spectrum. With further increase in pH, that is pH 4 and 6, PANI band at 3,150 cm^{-1} starts to merge with the band of sago starch at 3,303 cm^{-1}. Also, as the pH increases from 2 to 6, the intensity of absorption band at 3,150 cm^{-1} decreases, until it diminishes completely for the blends with pH 7 and above. This indicates deprotonation of PANI (from salt form to base form) in PANI/Sago blend with pH > 7, as no absorption band appears at 3,150 cm^{-1}. The absorption bands at 1,577 and 1,482 cm^{-1} attributed to quinonoid (Q) and benzenoid (B) ring-stretching vibrations (Furukawa et al., 1988; Ping, 1996) are observed in the spectrum of neat PANI (protonated salt form). For P/S 2 blend, the bands at 1,577 and 1,482 cm^{-1} of PANI blue shifts to 1,590 and 1,507 cm^{-1} and merges with bands at 1,644 and 1,420 cm^{-1} of Sago starch and broadens, as observed in **Figure 5**. The broadening and merging of bands is an indication of interaction between PANI and Sago, in this case its hydrogen bonding. However, on increasing the pH of PANI/Sago blends to ≥7, the bands at 1,577 and 1,482 cm^{-1} of PANI disappeared. The disappearance of these bands is another indication of deprotonation of PANI, as bands at 1,577 and 1,482 cm^{-1} denotes the oxidation state of PANI (Neelgund and Oki, 2011). Similar phenomenon was observed for band at 1,155 cm^{-1} of neat PANI, which is assigned to the vibration mode of the $–NH^{+}=$ structure, and is associated with the vibrations of the charged polymer units $Q = NH^{+}$-B or B–$NH^{+\bullet}$-B (Kang et al., 1998). The band at 1,155 cm^{-1} of neat PANI indicates the existence of positive charges on the chain and the distribution of the dihedral angle between the quinonoid and benzenoid rings. However, when PANI is synthesized in presence of Sago starch this band shifts to 1,110 cm^{-1}. For blends with pH ≤ 6 the absorption band at 1,110 cm^{-1} are intense and for blends with pH ≥ 7 the intensity reduces and merges with the absorption bands of Sago starch and ultimately resulting in broad absorption band, as shown in **Figure 5**. The shift and reduction in band intensity of absorption band at 1,155–1,110 cm^{-1} is due to the elimination of active site for charge transfer on the PANI backbone (MacDiarmid and Chiang, 1986; Tang et al., 1988). As this band has been related to the high degree of electron delocalization in PANI, as well as to a strong interchain $NH^{+}N$ hydrogen bonding (Trchová and Stejskal, 2011). Further, the most pronounced band at 805 cm^{-1} in the substitution region (900–650) cm^{-1} in the spectrum of neat PANI is due to the C–H out-of-plane bending vibrations of two adjacent hydrogen atoms on a 1,4-disubstituted benzene ring (Kang et al., 1998; Socrates, 2001). This confirms the dominating para-coupling of constitutional units in PANI chains. After the addition of NaOH to PANI/Sago dispersion, this band shifts to 760 cm^{-1} for all blends but P/S 11.

Overall, as observed in **Figure 5**, it was very difficult to pinpoint the changes in the spectrum at different pH, as some of the PANI peaks broadens and merges with the peaks of Sago starch, thus making it very difficult to differentiate. Nevertheless, it was noticed from **Figure 5**, that as the pH of the blends increases, the intensity of the PANI specific peaks (1,578, 1,490, 1,290, 1,240, 1,140, and 800 cm^{-1}) reduces and vice-versa for sago peaks (1,420 and 1644 cm^{-1}). The absorption peaks associated with the P/S 2 and P/S 4 spectrums, displays intense PANI-specific bands, the blends P/S 6 and P/S 7 were composed of low concentration of polyaniline incorporated in them, as evidenced by the low intensity of PANI characteristic bands and the PANI-specific bands almost disappeared or diminished for blends with pH 9 and 11. The characteristic bands at around 688, 1,644, and 3,303 cm^{-1} attributed to sago starch are present in all the blends but with varying intensities.

Morphology

The FE-SEM of neat PANI, neat Sago starch and the PANI/Sago blends of different pH are shown in **Figure 6**. **Figure 6A** is the FE-SEM of neat Sago starch, **Figure 6B** is the FE-SEM of neat PANI. Neat PANI shows the formation of cylindrical shaped nanostructures with an average diameter of 250 nm. The roughness observed on the PANI surface is attributed to doping process (John et al., 2010). For PANI/Sago blends it is difficult to demonstrate discrete PANI and Sago by FE-SEM analysis, suggesting a very fine distribution of PANI in the Sago starch, as shown in **Figures 6C–H**. For PANI/Sago blends at different pH, distinct morphologies were observed. Blends P/S 2 and P/S 4, displayed a coral-like morphology with small voids. The voids are indication of Sago degradation, as seen in **Figures 6C,D**. Blends P/S 6 and P/S 7, displays a highly connected morphology which helps in good inter and intra-chain electron transfer within the blends, as seen in **Figures 6E,F**. The morphology of the blends P/S 9 and P/S 11 also appears to be well-connected but with the presences of loose flakes in it. The flake like morphology could be a result of excess quantity of NaOH in PANI/Sago dispersion which resulted in deposition of NaCl salt on the PANI/Sago films. These results are in agreement with those reported in literature (Jelmy et al., 2013).

CONCLUSION

PANI/Sago films of varying pH (2–11) was successfully prepared using ultrasonic irradiation technique. The physical assessment of the films reveals at low pH (2 and 4) and high pH (9 and 11) Sago was degraded and resulted in brittle, spongy and shrunk films. The film obtained for pH 6 was found to be smooth, intact and ductile in nature. The degradation of Sago at low pH was further confirmed by proton NMR results, while also revealing deprotonation of PANI with the increase in pH > 7. The deprotonation of PANI was reflected in the E.C results, which showed gradual decrease in conductivity until pH 7 and then a drastic drop was noticed for pH 9 and 11. UV-Vis findings supports the phenomenon of PANI

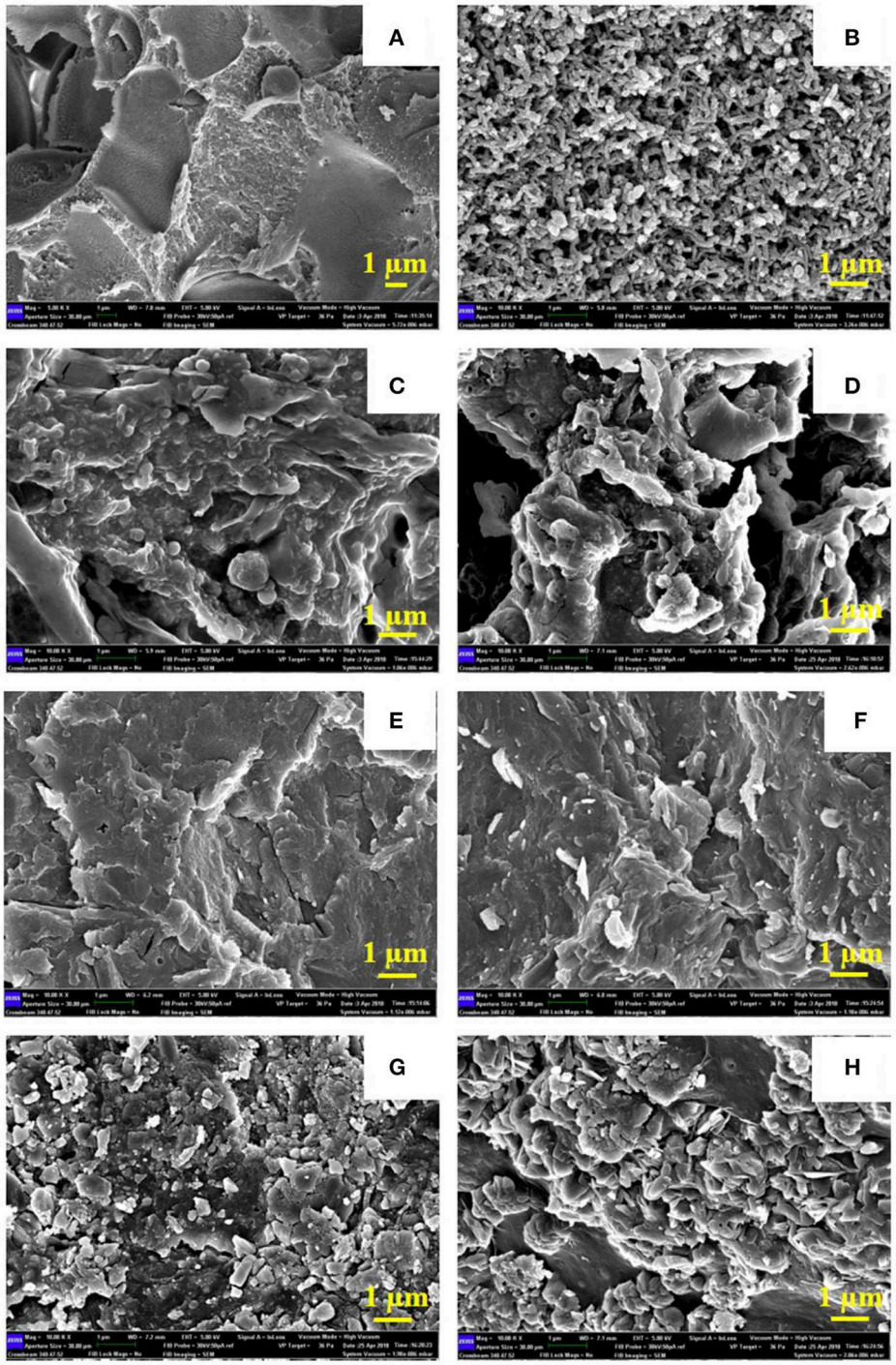

FIGURE 6 | FE-SEM of PANI, Sago, and PANI/Sago blends of varying pH. **(A)** Neat Sago. **(B)** Neat PANI. **(C)** P/S 2. **(D)** P/S 4. **(E)** P/S 6. **(F)** P/S 7. **(G)** P/S 9. **(H)** P/S 11.

deprotonation and also revealed, with the increase in pH, PANI deprotonates from emeraldine salt form to emeraldine base form. The effect of pH on the FT-IR spectrum of the blends was mostly in-differentiable, however it was found that P/S 6 blend was protonated and chemically stable compared to other blends. The morphological results were complimentary with ^{1}H NMR and FT-IR, while revealing different morphologies: coral like morphology with voids was observed for P/S 2 and P/S 4 blends; well-connected and smooth morphology was observed for P/S 6 and P/S 7 blend; and well-connected but with loose flakes was observed for P/S 9 and P/S 11 blend. Overall, the PANI/Sago blend P/S 6 was found to be electrically conductive

and physically stable. Apart from pH, the degradation of sago starch in the PANI/Sago blend could also be due to the kinetic energy exerted by sonication process. Therefore, the exact reason for degradation of Sago starch can be concluded conclusively only after studying the effect of sonication (reaction time) on the PANI/Sago blends.

DATA AVAILABILITY STATEMENT

All datasets generated for this study are included in the article/supplementary material.

AUTHOR CONTRIBUTIONS

MA and AA contributed conception and design of the study, conducted the experiments, collecting and analyzed the data, and also wrote the manuscript. NS organized the results and provided an explanation for the analysis of the section of physical assessment and morphological characteristics. NB helped MEAM to perform an analysis and discussion for the section of NMR and FTIR results. AH provided a proofread and provided a discussion for FTIR and NMR. All authors contributed to manuscript revision, read, and approved the submitted version.

REFERENCES

Abdelkader, R., Amine, H., and Mohammed, B. (2013). 1H-NMR spectra of conductive, anticorrosive and soluble polyaniline exchanged by an eco-catalyst layered (Maghnite-H+). *World Chem. J.* 2, 86–92. doi: 10.5829/idosi.wjc.2013.8.1.2902

Al-Thani, N., Hassan, M. K., and Bhadra, J. (2018). Polyaniline/polystyrene blends: in-depth analysis of the effect of sulfonic acid dopant concentration on ac conduct ivity using broadband dielectric spectroscopy. *Int. J. Polymer Sci.* 2018:1416531. doi: 10.1155/2018/1416531

Arenas, M., Sanchez, G., Martinez-Alvarez, O., and Castano, V. M. (2014). Electrical and morphological properties of polyaniline–polyvinyl alcohol *in situ* nanocomposites. *Comp. B* 56, 857–861. doi: 10.1016/j.compositesb.2013.09.010

Arrieta, A., Ganan, P., Marquez, S., and Zuluaga, R. (2011). Electrically conductive bioplastics from cassava starch. *J. Braz. Chem. Soc.* 22, 1170–1176. doi: 10.1590/S0103-50532011000600024

Beau, B., Travers, J., and Banka, E. (1999). NMR evidence for heterogeneous disorder and quasi-1D metallic state in polyaniline CSA. *Synthetic Metals* 101, 772–775. doi: 10.1016/S0379-6779(98)00357-9

Biswas, A., Shogren, R., Selling, G., Salch, J., Willett, J., and Buchanan, C. (2008). Rapid and environmentally friendly preparation of starch esters. *Carbohydr. Polymers* 74, 137–141. doi: 10.1016/j.carbpol.2008.01.013

Borah, R., Banerjee, S., and Kumar, A. (2014). Surface functionalization effects on structural, conformational, and optical properties of polyaniline nanofibers. *Synthetic Metals* 197, 225–232. doi: 10.1016/j.synthmet.2014.08.018

Cao, Y., Andreatta, A., Heeger, A., and Smith, P. (1989). Influence of chemical polymerization conditions on the properties of polyaniline. *Polymer* 30, 2305–2311. doi: 10.1016/0032-3861(89)90266-8

De Albuquerque, J., Mattoso, L., Faria, R., Masters, J., and MacDiarmid, A. (2004). Study of the interconversion of polyaniline oxidation states by optical absorption spectroscopy. *Synth. Metals* 146, 1–10. doi: 10.1016/j.synthmet.2004.05.019

Diop, C. I. K., Li, H., Xie, B., and Shi, J. (2011). Effects of acetic acid/acetic anhydride ratios on the properties of corn starch acetates. *Food Chem.* 126, 1662–1669. doi: 10.1016/j.foodchem.2010.12.050

Epstein, A., Joo, J., Kohlman, R., Du, G., MacDiarmid, A., Oh, E. J., et al. (1994). Inhomogeneous disorder and the modified Drude metallic state of conducting polymers. *Synthet. Metals* 65, 149–157. doi: 10.1016/0379-6779(94)90176-7

Fryczkowska, B., Piprek, Z., Sieradzka, M., Fryczkowski, R., and Janicki, J. (2017). Preparation and properties of composite PAN/PANI membranes. *Int. J. Polymer Sci.* 2017, 1–14. doi: 10.1155/2017/3257043

Furukawa, Y., Ueda, F., Hyodo, Y., Harada, I., Nakajima, T., and Kawagoe, T. (1988). Vibrational spectra and structure of polyaniline. *Macromolecules* 21, 1297–1305. doi: 10.1021/ma00183a020

Gill, E., Arshak, A., Arshak, K., and Olga, K. (2007). pH sensitivity of novel PANI/PVB/PS3 composite films. *Sensors* 7, 3329–3346. doi: 10.3390/s7123329

Gulrez, S., Ali Mohsin, M., Shaikh, H., Anis, A., Pulose, A., Yadav, M., et al. (2014). A review on electrically conductive polypropylene and polyethylene. *Polymer Comp.* 35, 900–914. doi: 10.1002/pc.22734

Huang, L., Wang, Z., Wang, H., Cheng, X., Mitra, A., and Yushan, Y. (2002). Polyaniline nanowires by electropolymerization from liquid crystalline phases. *J. Mater. Chem.* 12, 388–391. doi: 10.1039/b107499g

Huang, W., and MacDiarmid, A. (1993). Optical properties of polyaniline. *Polymer* 34, 1833–1845. doi: 10.1016/0032-3861(93)90424-9

Huang, W. S., Humphrey, B. D., and MacDiarmid, A. G. (1986). Polyaniline, a novel conducting polymer. Morphology and chemistry of its oxidation and reduction in aqueous electrolytes. *J. Chem. Soc.* 82, 2385–2400. doi: 10.1039/f19868202385

Janaki, V., Vijayaraghavan, K., Oh, B. T., Lee, K. J., Muthuchelian, K., Ramasamy, A., et al. (2012). Starch/polyaniline nanocomposite for enhanced removal of reactive dyes from synthetic effluent. *Carbohydr. Polymers* 90, 1437–1444. doi: 10.1016/j.carbpol.2012.07.012

Jelmy, E., Ramakrishnan, S., Devanathan, S., Rangarajan, M., and Nikhil, K. (2013). Optimization of the conductivity and yield of chemically synthesized polyaniline using a design of experiments. *J. Appl. Polymer Sci.* 130, 1047–1057. doi: 10.1002/app.39268

John, A., Mahadeva, S. K., and Kim, J. (2010). The preparation, characterization and actuation behavior of polyaniline and cellulose blended electro-active paper. *Smart Mater. Struct.* 19:045011. doi: 10.1088/0964-1726/19/4/045011

Jones, W. E., Chiguma, J., Johnson, E., Pachamuthu, A., and Daryl, S. (2010). Electrically and thermally conducting nanocomposites for electronic applications. *Materials* 3, 1478–1496. doi: 10.3390/ma3021478

Kang, E., Neoh, K., and Tan, K. (1998). Polyaniline: a polymer with many interesting intrinsic redox states. *Progr Polymer Sci.* 23, 277–324. doi: 10.1016/S0079-6700(97)00030-0

Kanungo, M., Kumar, A., and Contractor, A. (2003). Microtubule sensors and sensor array based on polyaniline synthesized in the presence of poly (styrene sulfonate). *Anal Chem.* 75, 5673–5679. doi: 10.1021/ac034537h

Kawano, K., Pacios, R., Poplavskyy, D., Nelson, J., Bradley, D., and James, D. (2006). Degradation of organic solar cells due to air exposure. *Solar Energy Mater. Solar Cells* 90, 3520–3530. doi: 10.1016/j.solmat.2006.06.041

Kohlman, R., Joo, J., Min, Y., MacDiarmid, A., and Epstein, A. (1996). Crossover in electrical frequency response through an insulator-metal transition. *Phys. Rev. Lett.* 77:2766. doi: 10.1103/PhysRevLett.77.2766

Kumar, A., Kumar, V., and Awasthi, K. (2018). Polyaniline–carbon nanotube composites: preparation methods, properties, and applications. *Polymer Plastics Technol. Eng.* 57, 70–97. doi: 10.1080/03602559.2017.1300817

Laska, J., Zak, K., and Pron, A. (1997). Conducting blends of polyaniline with conventional polymers. *Synth Metals* 84, 117–118. doi: 10.1016/S0379-6779(97)80673-X

Li, W., and Wang, H. L. (2004). Oligomer-assisted synthesis of chiral polyaniline nanofibers. *J. Am. Chem. Soc.* 126, 2278–2279. doi: 10.1021/ja039672q

Lindfors, T., and Ivaska, A. (2002). pH sensitivity of polyaniline and its substituted derivatives. *J. Electroanal. Chem.* 531, 43–52. doi: 10.1016/S0022-0728(02)01005-7

Lu, J., Moon, K., Kim, B., and Wong, C. (2007). High dielectric constant polyaniline/epoxy composites via *in situ* polymerization for embedded capacitor applications. *Polymer* 48, 1510–1516. doi: 10.1016/j.polymer.2007.01.057

Lu, X., Mao, H., Chao, D., Zhang, W., and Wei, Y. (2006). Fabrication of polyaniline nanostructures under ultrasonic irradiation: from nanotubes to nanofibers. *Macromol. Chem. Phys.* 207, 2142–2152. doi: 10.1002/macp.200600424

Lukasiewicz, M., Ptaszek, P., Ptaszek, A., and Szczepan, B. (2014). Polyaniline–starch blends: Synthesis, rheological, and electrical properties. *Starch Stärke* 66, 583–594. doi: 10.1002/star.201300147

MacDiarmid, A., and Chiang, J. (1986). Polyaniline': protonic acid doping of the emeraldine form to the metallic regime. *Synth. Metal* 13, 193–205. doi: 10.1016/0379-6779(86)90070-6

Neelgund, G. M., and Oki, A. (2011). A facile method for the synthesis of polyaniline nanospheres and the effect of doping on their electrical conductivity. *Polymer Int.* 60, 1291–1295. doi: 10.1002/pi.3068

Negi, Y. S., and Adhyapak, P. V. (2002). Development in polyaniline conducting polymers. *J. Macromol. Sci. C* 42, 35–53. doi: 10.1081/MC-120003094

Nguyen, H., Nguyen, T., Hoang, N., Le, N., Nguyen, T., Doan, D., et al. (2014). pH sensitivity of emeraldine salt polyaniline and poly (vinyl butyral) blend. *Adv. Nat. Sci.* 5:045001. doi: 10.1088/2043-6262/5/4/045001

Ning, Y. (2000). *Structural Identification of Organic Compounds and Organic Spectroscopy*. Beijing: Publishing Company of Science.

Persaud, K. C. (2005). Polymers for chemical sensing. *Materials Today* 8, 38–44. doi: 10.1016/S1369-7021(05)00793-5

Ping, Z. (1996). *In situ* FTIR–attenuated total reflection spectroscopic investigations on the base–acid transitions of polyaniline. Base–acid transition in the emeraldine form of polyaniline. *J. Chem. Soc. Faraday Transact.* 92, 3063–3067. doi: 10.1039/FT9969203063

Pour-Ali, S., Dehghanian, C., and Kosari, A. (2014). *In situ* synthesis of polyaniline–camphorsulfonate particles in an epoxy matrix for corrosion protection of mild steel in NaCl solution. *Corrosion Sci.* 85, 204–214. doi: 10.1016/j.corsci.2014.04.018

Pron, A., Genoud, F., Menardo, C., and Nechtschein, M. (1988). The effect of the oxidation conditions on the chemical polymerization of polyaniline. *Synth. Metals* 24, 193–201. doi: 10.1016/0379-6779(88)90257-3

Roichman, Y., Titelman, G., Silverstein, M., Siegmann, A., and Narkis, M. (1999). Polyaniline synthesis: influence of powder morphology on conductivity of solution cast blends with polystyrene. *Synth. Metals* 98, 201–209. doi: 10.1016/S0379-6779(98)00190-8

Saikia, J., Banerjee, S., Konwar, B., and Ashok, K. (2010). Biocompatible novel starch/polyaniline composites: characterization, anti-cytotoxicity and antioxidant activity. *Colloids Surf B* 81, 158–164. doi: 10.1016/j.colsurfb.2010.07.005

Shacklette, L. (1994). Dipole and hydrogen-bonding interactions in polyaniline: a mechanism for conductivity enhancement. *Synth. Metals* 65, 123–130. doi: 10.1016/0379-6779(94)90173-2

Socrates, G. (2001). *Infrared and Raman Characteristic Group Frequencies, 3rd Edn.* Hoboken, NJ: John Wiley & Sons.

Soetaredjo, F., Ismadji, S., Huynh, L., Kasim, N., Tran-Thi, N., Ayucitra, A., et al. (2012). Facile preparation of sago starch esters using full factorial design of experiment. *Starch Stärke* 64, 590–597. doi: 10.1002/star.201100169

Tang, J., Jing, X., Wang, B., and Wang, F. (1988). Infrared spectra of soluble polyaniline. *Synth Metals* 24, 231–238. doi: 10.1016/0379-6779(88)90261-5

Trchová, M., and Stejskal, J. (2011). Polyaniline: the infrared spectroscopy of conducting polymer nanotubes (IUPAC Technical Report). *Pure Appl. Chem.* 83, 1803–1817. doi: 10.1351/PAC-REP-10-02-01

Venancio, E. C., Wang, P. C., and MacDiarmid, A. (2006). The azanes: a class of material incorporating nano/micro self-assembled hollow spheres obtained by aqueous oxidative polymerization of aniline. *Synth. Metals* 156, 357–369. doi: 10.1016/j.synthmet.2005.08.035

Wallace, G. G., Teasdale, P. R., Spinks, G. M., and Kane-Maguire, L. A. P. (2002). *Conductive Electroactive Polymers: Intelligent Materials Systems, 2nd Edn*. Boca Raton, FL: CRC Press. doi: 10.1201/9781420031898

Wang, H., Wen, H., Hu, B.in., Fei, G., Shen, Y., Sun, L., et al. (2017). Facile approach to fabricate waterborne polyaniline nanocomposites with environmental benignity and high physical properties. *Sci. Rep*. 7:43694. doi: 10.1038/srep43694

Wang, X., Sun, T., Wang, C., Wang, C. E., Zhang, W., and Wei, Y. (2010). 1H NMR determination of the doping level of doped polyaniline. *Macromol. Chem. Phys.* 211, 1814–1819. doi: 10.1002/macp.201000194

Wudl, F., Angus, R. Jr., Lu, F., Allemand, P., Vachon, D., Nowak, M., et al. (1987). Poly-p-phenyleneamineimine: synthesis and comparison to polyaniline. *J. Am. Chem. Soc.* 109, 3677–3684. doi: 10.1021/ja00246a026

Yamamoto, T., and Moon, D. K. (1993). 1H NMR spectra of polyanilines and dynamic exchange of NH hydrogen with H2O. Die Makromolekulare Chemie. *Rapid Commun.* 14, 495–501. doi: 10.1002/marc.1993.030140807

Zhang, X., Goux, W. J., and Manohar, S. K. (2004). Synthesis of polyaniline nanofibers by "nanofiber seeding". *J. Am. Chem. Soc.* 126, 4502–4503. doi: 10.1021/ja031867a

Zujovic, Z., Zhang, L., Bowmaker, G., Kilmartin, P., and Jadranka, T. (2008). Self-assembled, nanostructured aniline oxidation products: a structural investigation. *Macromolecules* 41, 3125–3135. doi: 10.1021/ma071650r

Conflict of Interest: The authors declare that the research was conducted in the absence of any commercial or financial relationships that could be construed as a potential conflict of interest.